Low-temperature Oxidation of Ammonia in Fixed and Fluidized Beds

H. F. Johnstone, J. D. Batchelor, and C. Y. Shen, University of Illinois, Urbana, Illinois

The oxidation of ammonia in the presence of manganous oxide-bismuth oxide catalyst supported on small alumina spheres was studied in both fixed and fluidized beds in the temperature range from 205° to 250°C. The column used was 4½ in. in diameter and 43 in. high. The experiments were made so that the transport effects in the fluidized bed might be separated from the chemical kinetic effects.

In accordance with the theory of two-phase fluidization proposed in a previous paper, comparison is made between the reaction rate associated with the discontinuous phase and that associated with the continuous phase as estimated from the results in the fixed bed. The over-all reaction-rate constants in the fluidized bed can be related to those in the fixed bed by an exponential term in the superficial gas velocity, V^n; n is a constant which depends on the reaction system and the size and type of the reactor.

Little information has been published on reaction kinetics in fluidized beds. Gilliland, Mason, and Oliver reported that at the same space velocity a fluidized bed gives a lower conversion for a homogeneous gas reaction than does a fixed bed (*4*). This was attributed to mixing and by-passing in the bed. On the basis of pressure drop studies, Toomey and Johnstone (*10*) suggested that a fluidized bed may be considered to be composed of two phases: a continuous phase consisting of uniformly dispersed particles in a supporting gas stream and a discontinuous phase consisting of pure gas in the form of bubbles, channels, or slugs. On this basis an equation was developed for the variation of pressure drop with gas velocity.

In a fluidized catalytic reactor the two-phase concept implies that the type and degree of contact between the gas and solid will be completely different for the two phases. For the most part the gas in the continuous phase supports the catalyst particles and flows through the interstices in a manner analogous to the flow in a fixed bed. As the rate of flow of gas in the continuous phase is limited by the formation of the discontinuous phase, the flow in this phase is always laminar, at least for beds of small spherical particles. For a given bed the reaction rate in the continuous phase should depend on molecular diffusivities and be independent of the presence of the discontinuous phase. The actual concentrations of the reactants, however, will usually depend on the rate of transfer between the phases, which will be affected by the motion of the discontinuous phase.

In general there will be some supplementary reaction in the discontinuous phase, or at the phase boundary, which cannot be assigned definitely to the continuous phase. At the point of incipient two-phase fluidization, however, all the reaction may be assigned to the continuous phase; any increase in reaction rate at higher gas velocities must be associated directly or indirectly with the discontinuous phase. It will be interesting to apply this concept to actual kinetic data and to develop a method of estimating the rate in a fluidized bed from the constants obtained for a fixed bed.

The reaction used for studying the effect of fluidization on the re-

J. D. Batchelor's present address is Pittsburgh Consolidation Coal Company, Library, Pennsylvania; C. Y. Shen is with Monsanto Chemical Company, Dayton, Ohio.

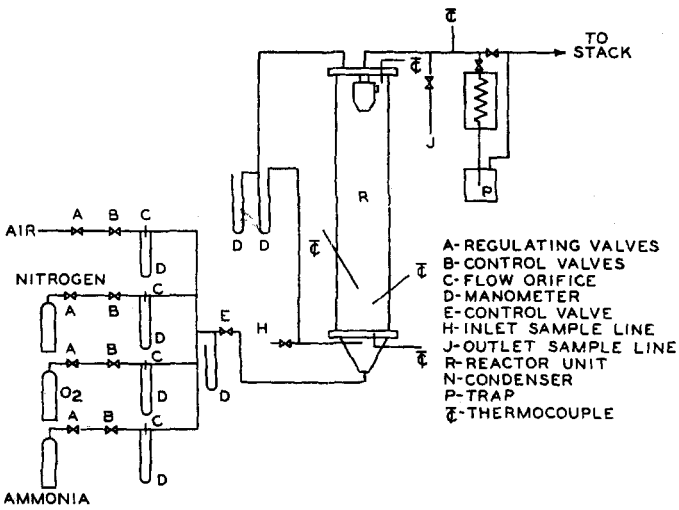

Fig. 1. Flow diagram of experimental equipment.

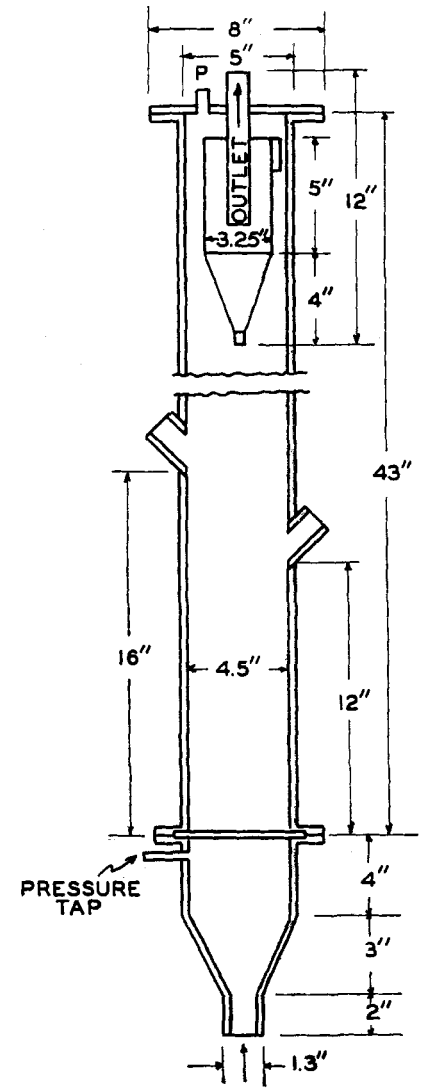

Fig. 2. Fluidized-bed unit.

TABLE 1.—PROPERTIES OF CATALYST FRACTIONS

Fraction	Geometric mean diameter, μ	Geometric standard deviation	Particle density,* g./cc.	Apparent density, g./cc.	%MnO (dry basis)	%Bi_2O_3 (dry basis)
165-200 mesh	103	1.19	2.08	1.10	3.51	3.75
120-165 mesh	139	1.14	2.05	1.05	3.48	3.63
+120 mesh	178	1.23	2.01	1.00	3.43	3.51
Unsized	103	1.36	2.06	1.08	4.20	4.15

*By displacement of mercury.

action kinetics in a fluidized bed was the low-temperature oxidation of ammonia. This reaction has been investigated thoroughly in a tubular reactor(*5*), and the catalyst, manganous oxide and bismuth oxide, was shown to have a constant activity over several hundred hours.

The mechanism of ammonia oxidation of temperatures around 1,000°C. has been studied by Bodenstein(*2*) and Zawadzki(*11*). At lower temperatures, in the range from 200° to 300°C., Nagel(*9*) found that nitrous oxide is the principal product of the reaction. A more detailed study with metallic oxide catalysts was made by Krauss(*8*). In a fixed bed of manganous oxide–bismuth oxide, Kobe and Hosman(*7*) obtained a maximum yield of 71% nitrous oxide in the temperature range from 175° to 300°C. at space velocities of 3.5 to 6 min.$^{-1}$ The mechanism studies at low temperatures in the tubular reactor(*5*) showed that the rate depends on the amount of adsorbed oxygen on the catalyst and the concentration of ammonia in the gas phase.

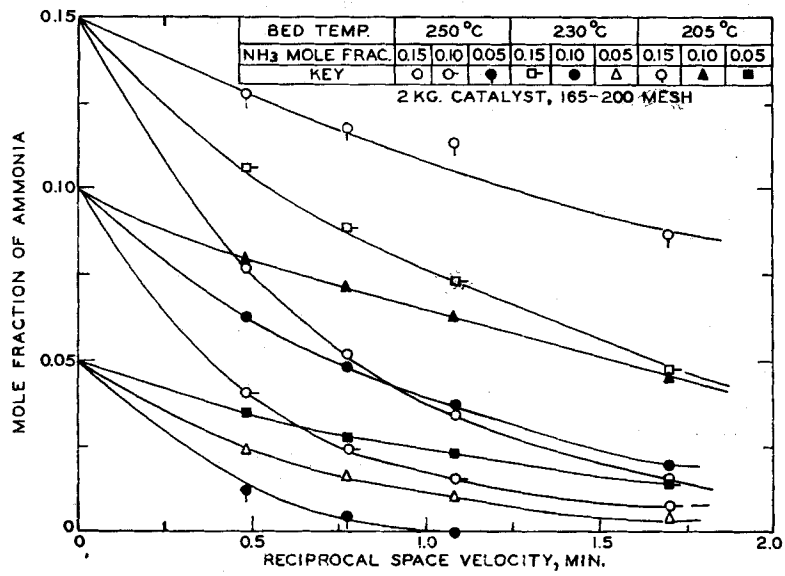

Fig. 3. Effect of temperature, concentration, and contact time on ammonia oxidation in fixed-catalyst beds.

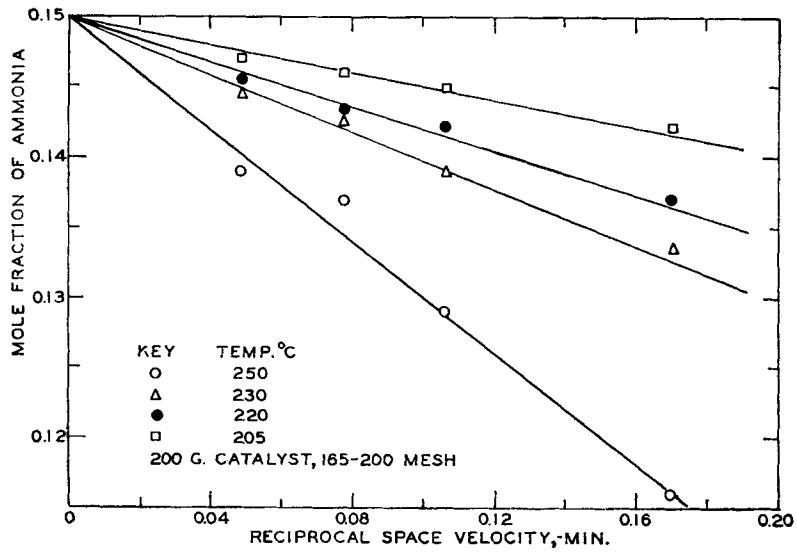

Fig. 4. Effect of temperature on oxidation rate at high ammonia concentration and low contact time in fixed beds.

EXPERIMENTAL

Apparatus

The equipment used is shown in Figure 1. The flow of cylinder gases was regulated with ½-in. needle valves and measured through calibrated sharp-edged flowmeters. The reactor, 4½ in. I. D. and 43 in. high, was constructed from type-310 stainless steel. The lower flange was connected to a conical inlet section and held a stainless steel porous plate which supported the bed and distributed the gas flow uniformly. The upper flange supported the cyclone separator for removing the catalyst particles from the gas. The small amount of catalyst collected in the cyclone was returned to the reactor at the end of each series of runs. Details of the reactor are shown in Figure 2. It was heated by six 750-watt Chromalox resistance strip heaters which were controlled automatically. Later the heaters were replaced by three sections of chromel ribbon wound on alundum insulation to give more uniform temperature distribution. Temperatures of the fluidized bed were measured by two iron-constantan thermocouples in stainless steel wells located in the axis of the column. Thermocouples were also installed on the porous plate and on the reactor walls near the geometric centers of the heated sections. The exit gas lines were heated electrically to prevent condensation of water.

Catalyst

The catalyst was made by impregnation of Alcoa XF-21-Si (low soda) alumina fluid-cracking catalyst. One kilogram of the alumina particles was first dampened with 250 cc. of a solution containing 100 g. manganous nitrate and 35 g. bismuth nitrate. The impregnated catalyst was dried in a steam heated vacuum oven for 5 days prior to heating in a large electric furnace at 375°C. for 2 days. Part of the dried catalyst was separated by sieving on 120-, 165-, and 200-mesh screens. Final size distributions in each fraction were determined by measuring 300 particles under a microscope. The geometric mean diameters, standard deviations, and other properties of the catalysts are shown in Table 1. The catalyst particles were generally smooth and rounded but not truly spherical.

Procedure

Before a reaction run was made, a weighed portion (3 to 6 kg.) of one

of the impregnated catalyst fractions was placed in the reactor through the top of the column, which was then heated to the reaction temperature while the bed was fluidized with air. When the reaction temperature was reached and the temperature controller was operating smoothly, a series of measurements was made on the pressure drop across the bed; the air rate was started much higher than required to fluidize the bed and was reduced in steps to a value below the fluidization rate. The pressure-drop curve was determined by decreasing the air rate to avoid any static friction effects near the minimum fluidization point.

The oxygen-ammonia gas stream was then substituted for the air flow. At least 2 hrs. was allowed for the attainment of steady state. The gauge pressure at the bed outlet was set at about 9 cm. of water, and the absolute pressure at E (Figure 1) was regulated to 820 mm. Hg. Simultaneous inlet and outlet gas samples were drawn through weighed tubes of magnesium perchlorate and Ascarite for the determination of water vapor, ammonia, and nitrogen peroxide(*5*). The volumes of gas sampled at the rate of about 0.01 cu.ft./min. were measured with wet test meters. The oxygen and ammonia flow rates, the pressure drop across the bed, the orifice downstream pressure, and the temperature were also noted.

A sample of the gas leaving the absorption tubes was mixed with a measured volume of pure hydrogen in an Orsat-type gas burette and the oxygen content determined by absorption in Oxsorbent. The nitrous oxide was then reacted with the hydrogen in a slow combustion pipette, and the decrease in volume was equivalent to the volume of nitrous oxide present. Nitrogen was determined from the volume of the remaining gas.

RESULTS IN FIXED-BED REACTOR

In the low-temperature oxidation of ammonia, several simultaneous reactions can occur to give various products. In order to interpret the results in the fluidized bed, experiments were made at low gas velocities in the same apparatus under the same conditions but with the catalyst stationary. A gas mixture containing 10% ammonia and 90% oxygen was first passed at various rates through the empty reactor at 250°C. to determine whether the metallic surface of the reactor wall and the porous support might have some catalytic effect. No reaction took place under these conditions.

The results obtained with a bed of 2 kg. of 165- to 200-mesh catalyst at 250°, 230°, and 205°C. at different space velocities are shown in Figure 3. At high temperatures and low gas velocities the extent of conversion is high and the possible error is greater than it is at low temperatures and low velocities.

To overcome the high conversion at high temperatures, the weight of catalyst was reduced to 200 g. The results at the higher space velocities are shown in Figure 4. For each temperature the rate of oxidation is independent of the concentration above 12% ammonia in the gas mixture. Thus under these conditions the reaction follows approximately an over-all zero-order process.

In a previous paper the mechanism of the low-temperature oxidation was shown to be a bimolecular surface reaction involving adsorbed oxygen atoms and ammonia diffusing to the surface(*5*). The reaction may be expressed by

$$NH_3 + [O]_{ads} \longrightarrow \text{intermediate} \longrightarrow \text{oxidized product} \qquad (1)$$

The suggested intermediates are hydronitrous acid, hydroxylamine, or imide(*2, 11*). The rate is represented by the equation

$$\frac{d(NH_3)}{d\tau} = k[O]_{ads}[NH_3] \qquad (2)$$

where τ is the reciprocal space velocity expressed as volume of catalyst per unit of volumetric gas-feed rate. The volume of the catalyst is obtained from the weight of catalyst in the bed and the absolute density shown in Table 1. The reciprocal space velocity obtained in this way differs from the conventional definition by a factor of $1/(1-\varepsilon)$, where ε is the void fraction. The expression can be extended to the fluidized region without the confusion of uncertain values of ε in the expanded catalyst bed. Furthermore, if a Langmuir type of isotherm describes the adsorption of oxygen, Equation (1) becomes

$$-\frac{d(NH_3)}{d\tau} = \frac{k'\sqrt{(O_2)}}{1+\sqrt{K(O_2)}}(NH_3) \qquad (3)$$

where K is the adsorption equilibrium constant. At atmospheric pressure the concentration of each reactant may be replaced by its respective partial pressure.

$$-\frac{dp_{NH_3}}{d\tau} = \frac{k' p_{NH_3}\sqrt{p_{O_2}}}{1+\sqrt{Kp_{O_2}}} \qquad (3a)$$

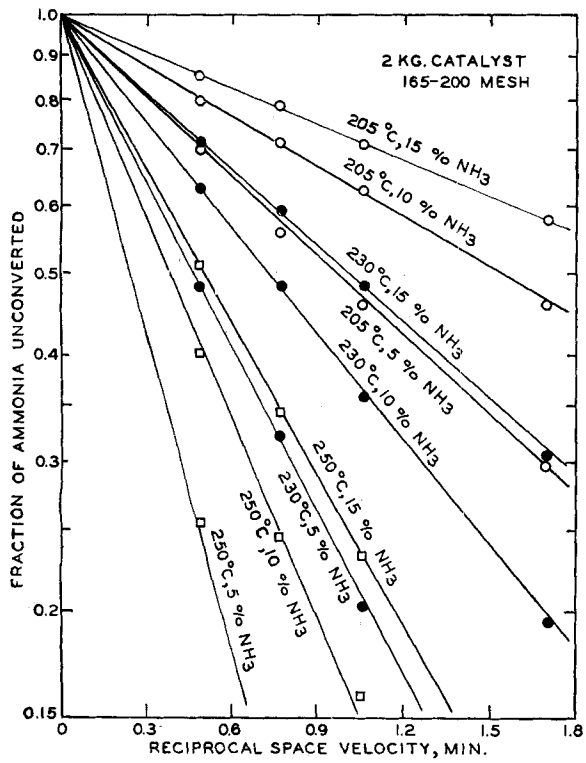

Fig. 5. Oxidation of ammonia following first-order reaction in fixed beds.

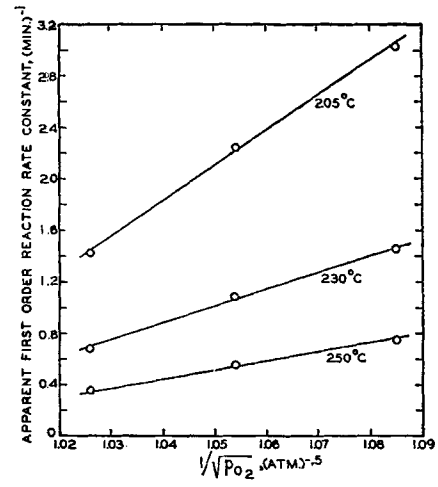

Fig. 6. Effect of temperature and oxygen pressure on apparent first-order reaction.

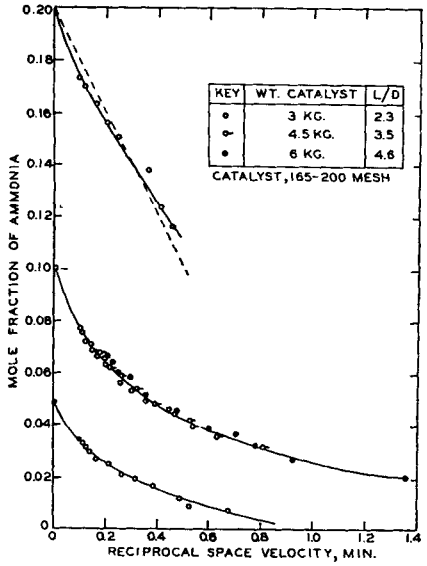

Fig. 7. Effect of initial concentration of NH_3 on oxidation rate at 250°C. in fluidized beds. Dotted line represents zero-order rate calculated from data for fixed-bed reactors.

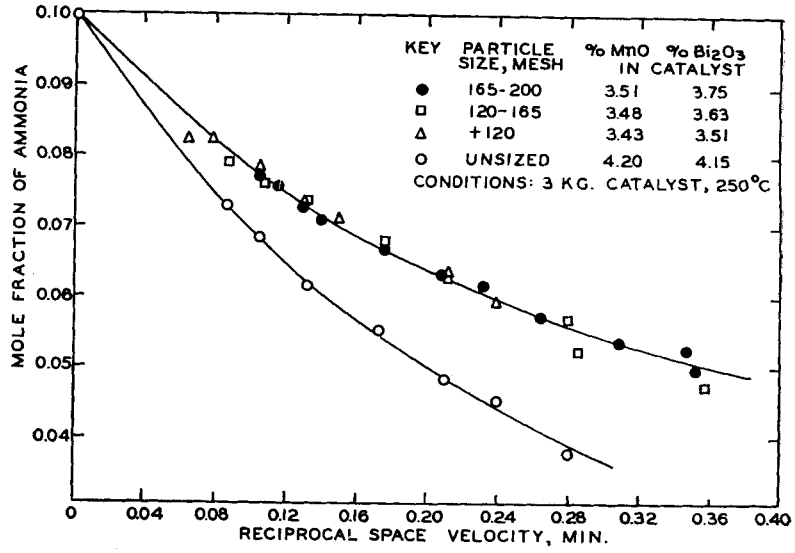

Fig. 8. Effect of catalyst size and composition on oxidation rate in fluidized beds.

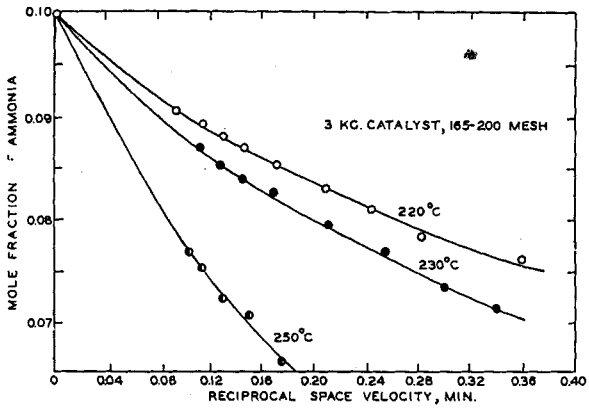

Fig. 9. Effect of temperature and contact time on oxidation rate in fluidized beds.

In the present work a high oxygen: ammonia ratio was used so that the concentration of oxygen remained essentially constant. Thus, Equation (3*a*) represents a pseudo first-order reaction which on integration becomes

$$\ln(1-\alpha) = -k'_1\tau \qquad (4)$$

where α is the fraction conversion. Figure 5 is a replot of the data in Figure 3, which show that the results are in agreement with the first-order equation. The rate constant k'_1 depends on the average partial pressure of oxygen as indicated by

$$k'_1 = \frac{k'\sqrt{p_{O_2}}}{1+\sqrt{Kp_{O_2}}} \qquad (4a)$$

A plot of $1/k'$ vs. $1/\sqrt{p_{O_2}}$ yields a straight line at a given temperature, as shown in Figure 6, from which the value of k' and the adsorption equilibrium constant can be determined. When the right-hand side of Equation (4) is small, $\exp(-k'_1\tau)$ can be expanded into a series and all terms except the first are negligible, or

$$\alpha = k'_1\tau \qquad (5)$$

It is this apparent zero-order reaction that is shown in Figure 4. At 250°C. k'_1 is 1.33 min.$^{-1}$ The error in $(1-\alpha)$ resulting from using only the first two terms of $\exp(-k'\tau)$ at τ equal to 0.2 min. is about 5%. Since the product yield in a zero-order process depends only on the time of contact with the catalyst, the reaction rate in this range is substantially the same in a fluidized bed as in a fixed bed under the same conditions.

RESULTS IN FLUIDIZED BEDS

The work on fluidized beds was carried out in the same apparatus but at higher gas velocities(*1*). The velocity for minimum fluidization was determined from pressure-drop measurements. The pressure drop was plotted against the gas velocity, and the sharp break extrapolated from the fixed- and fluidized-bed regions was assumed to be the minimum fluidization point.

The complete results of the kinetic studies, showing the effects of ammonia concentration, particle size of catalyst, and temperature on the reaction rate, are shown in Figures 7 to 9. The space velocity was calculated in the same way as for the fixed bed. The method does not differentiate between the bubbles of gas and the gas that supports the catalyst; however, it does allow a correlation of the data from fixed beds with those from fluidized beds. Increasing the bed depth maintained the same space velocity in the fluidized bed as was used for the fixed-bed studies. The effect of temperature is approximately the same as for the fixed bed, but the over-all conversion cannot be correlated with the first-order relationship of Equation (4). In Figure 7 the dotted line represents the zero-order rate determined from Figure 6 by use of the corresponding average partial pressure of oxygen.

The particle size of the catalyst does not have much effect on the reaction rate in the range from +120 to 165-200 mesh, as shown in Figure 8. The higher activity of the unsized catalyst may be caused by its higher content of active metallic oxides.

DISCUSSION OF RESULTS

The change in conversion rate in going from a fixed-bed to a fluidized reactor depends on the effect on the rate of chemical reaction and on the physical nature of

the gas-solid contact in the bed. If only a portion of the gas contacts the catalyst and the rest bypasses the bed in the form of bubbles, then the over-all rate depends on the rate of transfer from the discontinuous phase to the continuous phase in contact with the solids and on the rate of chemical reaction at the surface. If one assumes that the effective contact and the transfer rate between the gas and the catalyst particles may be expressed as an exponential function of the gas velocity, the over-all rate constant for the fluidized bed for a constant temperature becomes

$$k'_f = AV^n \qquad (6)$$

The constant A is related to the fixed-bed reaction-rate constant, because when the velocity approaches that of minimum fluidization, the rate constant defined by Equation (6) should agree with the value obtained from the fixed bed. Then

$$k'_1 = AV_{mf}^n \qquad (7)$$

and

$$\frac{k'_f}{k'_1} = \left(\frac{V}{V_{mf}}\right)^n \qquad (8)$$

Substitution of Equation (6) into the first-order rate equation gives

$$-\frac{dp_{NH_3}}{d\tau} = AV^n(p_{NH_3}) \qquad (9)$$

This involves the assumptions that the over-all rate is proportional to the partial pressure of ammonia in the gas, and the partial pressure of oxygen remains constant in the reactor.

Since $\tau = W/\rho V$, integration under isothermal and isobaric conditions gives

$$\int_p^{p(1-\alpha)} \frac{dp}{p} = \frac{AW}{\rho}\int_\infty^V V^{n-2}dV \qquad (10)$$

If n is less than one, then

$$\ln(1-\alpha) = \frac{AW}{\rho(n-1)}V^{n-1} \qquad (11)$$

A plot of $-\ln(1-\alpha)$ vs. the volumetric gas velocity on a logarithmic scale is shown in Figure 10. In the fluidized range of velocities, the lines are parallel. From the slope, the value of n is 0.17. Since n is positive, the reaction rate is faster in the fluidized bed than in the fixed bed at the same space velocity. A similar conclusion was reached by Kivnick and Hixson(*6*) for the reduction of nickel oxide in a fluidized bed, although no measurements were made in the fixed-bed region. The value of n obtained by them was approximately 0.70. Thus n is determined by the nature of the gas-solid reaction, but it appears to be independent of particle size, as shown in Figure 10.

For reactions that are not zero order, either by-passing of the gas as bubbles or mixing of the gas in the fluidized bed will result in a lower reaction rate in a fluidized reactor than in a fixed bed. Although the mass transfer constant in a fluidized bed was found by Chu(*3*), it is not possible to draw the conclusion that the reaction mechanism in a fluidized bed is changed to a diffusion — controlling step. The vigorous movement of particles inside a fluidized bed may also increase the effectiveness of the particle surface for a chemical reaction.

The relative values of A estimated from the intercepts in Figure 10 are shown in Figure 11 together with the reaction-rate constants from the fixed-bed data. The activation energy obtained from the slope of the lines is 14.8 kcal./g. mole. It is the same as for the fixed bed when the same catalyst is used.

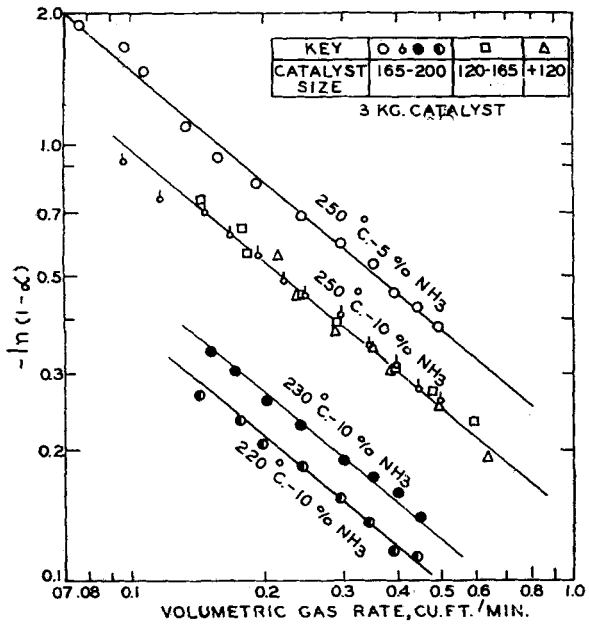

← Fig. 10. Effect of gas velocity on conversion rate in fluidized beds.

TWO-PHASE FLUIDIZATION THEORY

The concept of two-phase fluidization may be used to explain the observed kinetic data. When the gas rate is sufficient to produce two-phase fluidization, the total reaction is the sum of that in each phase. From the flow characteristics alone, the formation of the discontinuous phase is expected to decrease the over-all percentage conversion. However, if there is mass transfer between the phases, or any supplementary reaction in the discontinuous phase, the over-all rate may increase. The increase in pressure drop with gas velocity above the point of two-phase fluidization(*10*) is given by

$$\frac{\Delta p_{ke}}{\Delta p_{mf}} = (lD_p^{0.5} - m)\ln\frac{V}{V_v} \qquad (12)$$

Δp_{ke} is the kinetic-energy loss caused by bubbles of the discontinuous phase passing through the continuous phase. This should also be a measure of the degree of contact of the two phases, and the effect of the discontinuous phase on the reaction rate should in a similar manner depend on the flow rate.

The pressure-drop measurements showed that the flow rate at minimum fluidization is 70 to 85% of the value at incipient two-phase fluidization. Since there was no way of observing the initial formation of the second phase in the reactor, the lower value was used

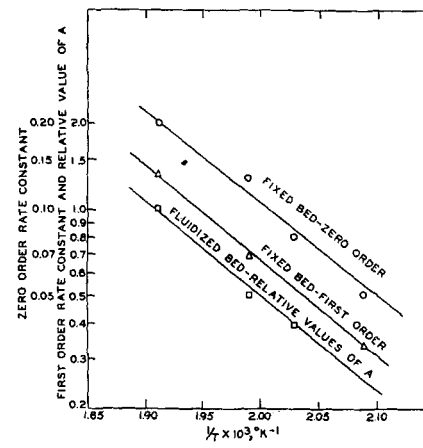

Fig. 11. Variation of reaction-rate constants with temperature.

to estimate the flow rate at which the discontinuous phase was just formed in the kinetic studies. The corresponding value of the fractional conversion, α_c, was found from Figures 7 and 9 and the rate of reaction in the continuous phase was calculated from

$$R_c = (\alpha_c)\,(V_v)\,(y_1) \qquad (13)$$

The reaction rate in the discontinuous phase was then found from

$$R_d = R - R_c \qquad (14)$$

The ratios R_d/R_c for all the data obtained with the fluidized bed are plotted in Figure 12. The lines are represented by

$$\frac{R_d}{R_c} = K_s \log \frac{V}{V_v} \qquad (15)$$

The slopes and intercepts evaluated by the method of least squares are shown in Table 2.

For the pressure-drop data, the slope of the $\Delta p_{ke}/\Delta p_{mf}$ vs. log V lines is a function of $Dp^{0.5}$ (*10*). A slight effect of the size of the column was also noted, as was to be expected. For the reaction-rate data, the effect of particle size is quite different, since the surface area related to the reaction rates is not the same as that affecting the pressure drop. The reaction rate in the continuous phase should be directly proportional to the surface area per unit volume of the bed. Thus

$$R_c \propto \frac{6\,(1-\epsilon)}{D_p} \qquad (16)$$

At constant gas velocity the reaction rate in the discontinuous phase is determined by the surface area of the bubbles. It may be postulated that the initial size of the bubbles is proportional to the interstitial space between the particles. The bubbles initially formed coalesce and become larger as they ascend. Thus the bubble surface is proportional to D_p^{-2} or

$$\frac{R_d}{R_c} \propto \frac{1}{D_p} \qquad (17)$$

Since $\Delta p_{ke}/\Delta p_{mf}$ is proportional to $D_p^{0.5}$, then

$$\frac{R_d}{R_c} \propto D_p^{-1.5}\,\frac{\Delta p_{ke}}{\Delta p_{mf}} \qquad (18)$$

or

$$\frac{R_d}{R_c} \propto D_p^{-1} \ln \frac{V}{V_v} \qquad (19)$$

In a comparison of Equations (19) and (15), the slope K_s is seen to be inversely proportional to the diameter of the catalyst particles.

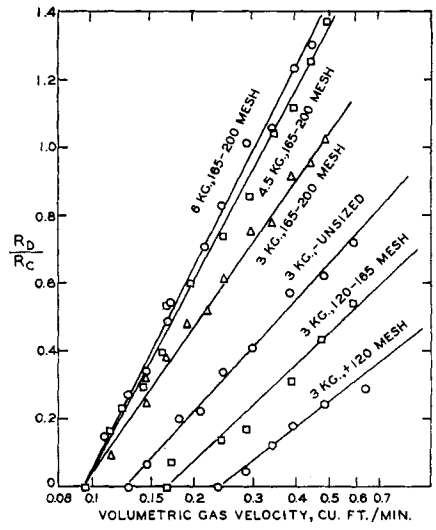

Fig. 12. Effect of gas velocity on reaction rates in discontinuous phase. Initial ammonia concentration 10%, 250°C.

TABLE 2.—VALUES OF THE CONSTANTS K_s AND V_v IN EQUATION (15)

Fluidized bed Weight, kg.	Size	K_s	Gas rate at incipient fluidization, V_v, std. cu.ft./min.
3	165-200 mesh	1.44	0.094
4.5	165-200 mesh	1.87	0.094
6	165-200 mesh	2.01	0.094
3	+120 mesh	0.73	0.238
3	120-165 mesh	0.97	0.173
3	unsized	1.09	0.125

CONCLUSIONS

The reaction rate at incipient fluidization can be estimated from the rate in the fixed bed; hence Equation (15) should be useful for estimating the reaction rate in a fluidized bed. Since the value of K_s undoubtedly depends on the type and size of reactor, this effect should be investigated with other reactions before Equation (15) can be accepted for general scale-up purposes. The results indicate that the reaction rate in a fluidized bed can be divided into two parts: the part that is related only to the chemical kinetics can be predicted from the rate in a fixed bed; the part that depends on mass transfer from the discontinuous phase is a function of the gas velocity and is independent of the particle size.

ACKNOWLEDGMENT

The authors express their appreciation to the Dupont Company for support of a graduate fellowship during part of the work, which was completed as part of the program of the Engineering Experiment Station.

NOTATION

A = a constant defined by Equation (6)
D_p = diameter of catalyst particle, ft.
k, k' = reaction-rate constants
k'_l = first-order rate constant, min.$^{-1}$
k'_f = reaction-rate constant in fluidized bed
K = adsorption equilibrium constant
K_s = slope defined by Equation (16)
l, m, n = constants
p = partial pressure; subscript NH_3 and O_2 denote ammonia and oxygen, respectively, atm.
Δp = pressure drop; subscript *mf* refers to incipient fluidization of *ke* to excess drop above fluidization, lb./sq.in.
R = conversion rate; subscript *c* refers to continuous phase, and *d* refers to discontinuous phase, lb.moles/min.
T = temperature, °K.
V = volumetric gas velocity; subscript *v* refers to incipient fluidization, cu.ft./min.
W = weight of catalyst, lb.
y = concentration of ammonia; subscript *l* refers to inlet, moles/cu.ft.

Greek Letters

α = fraction conversion
τ = reciprocal space velocity, min.
ρ = absolute density of catalyst, lb./cu.ft.
ϵ = void fraction

LITERATURE CITED

1. Batchelor, J. D., Ph.D. thesis, University of Illinois (1952).
2. Bodenstein, M., *Trans. Electrochem. Soc.*, 71, 353 (1937).
3. Chu, J. C., J. Kalil, and W. A. Wetteroth, *Chem. Eng. Progr.*, 49, 141 (1953).
4. Gilliland, E. R., E. A. Mason, and R. C. Oliver, *Ind. Eng. Chem.*, 45, 1177 (1953).
5. Johnstone, H. F., E. T. Houvouras, and W. R. Schowalter, *Ind. Eng. Chem.*, 46, 702 (1954).
6. Kivnick, A., and A. N. Hixson, *Chem. Eng. Progr.*, 48, 394 (1952).
7. Kobe, K. A., and R. D. Hosman, *Ind. Eng. Chem.*, 40, 397 (1948).
8. Krauss, W., *Z. Electrochem.*, 53, 320 (1949).
9. Nagel, A. V., *Z. Electrochem.*, 36, 754 (1930).
10. Toomey, R. D., and H. F. Johnstone, *Chem. Eng. Progr.*, 48, 220 (1952).
11. Zawadzki, J., *Discussions Faraday Soc.*, No. 8, 140 (1950).

(Presented at A.I.Ch.E. New York meeting)